

Field-induced breakdown of the quantum Hall effect

K. Shizuya

*Yukawa Institute for Theoretical Physics
Kyoto University, Kyoto 606-8502, Japan*

A numerical analysis is made of the breakdown of the quantum Hall effect caused by the Hall electric field in competition with disorder. It turns out that in the regime of dense impurities, in particular, the number of localized states decreases exponentially with the Hall field, with its dependence on the magnetic and electric field summarized in a simple scaling law. The physical picture underlying the scaling law is clarified. This *intraband* process, the competition of the Hall field with disorder, leads to critical breakdown fields of magnitude of a few hundred V/cm, consistent with observations, and accounts for their magnetic-field dependence $\propto B^{3/2}$ observed experimentally. Some testable consequences of the scaling law are discussed.

73.40.Hm, 73.20.Jc

I. INTRODUCTION

Since the discovery of the quantum Hall effect^{1–5} (QHE) there has been considerable interest in its breakdown^{6–13} due to high currents. Rich accumulation of experimental data has recently shed new light on this breakdown phenomenon: A series of experiments by Kawaji *et al.*¹¹ using butterfly-shaped Hall bars clearly showed that the breakdown of the QHE is controlled by the current density or the Hall field rather than the current itself and that for samples with a variety of electron concentration and mobility the critical values of the Hall field at different diagonal-resistance plateaus scale like $\propto B^{3/2}$ with the magnetic field B . This $B^{3/2}$ dependence disfavors some of the breakdown mechanisms proposed earlier, such as those attributed to electron heating⁶ and phonon emission.⁸ Zener tunneling^{8,14–17} of electrons across the Landau gap appears consistent with it but theoretically yields critical fields one order of magnitude larger than observed experimentally.

In a previous paper¹⁸ we presented a numerical study of current distributions in Hall bars. There we noted, as a by-product of the study, the possibility that the Hall field in competition with disorder in the sample interior would be responsible for the breakdown of the QHE, with a simple estimate of the competition that leads to critical fields of magnitude consistent with observations and their $B^{3/2}$ scaling law. The purpose of the present paper is to verify by a detailed numerical analysis that this *intraband* process can indeed account for the breakdown phenomenon. Actually Stormer *et al.*⁸ earlier noted that the action of a Hall field could qualitatively explain many of their experimental findings. Recently Shimada

*et al.*¹³ also suggested, through a measurement of activation energy, that the $B^{3/2}$ scaling law is related to field-dependent broadening of the spectra of extended states. We shall study numerically how the fraction of delocalized states per Landau subband depends on the electric and magnetic field and clarify the physical picture underlying the scaling law.

In Sec. II we review a theoretical framework¹⁸ for our numerical simulations. We examine the case of a single impurity in Sec. III and handle Hall samples with random impurities in Sec. IV. Section V is devoted to a summary and discussion.

II. FORMALISM

Consider electrons confined to a strip of length L_x and width L_y (or formally, a strip bent into a loop of circumference L_x), described by the Hamiltonian:

$$H = H_0 + U(x, y) - eA_0(y), \quad (2.1)$$

$$H_0 = \frac{1}{2}\omega \left\{ \ell^2 p_y^2 + (1/\ell^2)(y - y_0)^2 \right\}, \quad (2.2)$$

written in terms of $\omega \equiv eB/m$, the magnetic length $\ell \equiv 1/\sqrt{eB}$ and $y_0 \equiv p_x/(eB)$. Here a uniform magnetic field B normal to the plane has been introduced by use of the Landau-gauge vector potential $(-By, 0)$.

We shall detect the current $j_x(x, y)$ flowing in the presence of a Hall potential $A_0(y)$ and an impurity potential

$$U(x, y) = \sum_i \lambda_i \delta(x - x_i) \delta(y - y_i), \quad (2.3)$$

which consists of short-range impurities of strength λ_i distributed over the sample at position (x_i, y_i) . For simplicity, we here take $A_0(y) = -yE_y$ which produces a uniform Hall field E_y in the y direction.

The cyclotron motion of an electron is described by H_0 , whose eigenstates are Landau levels $|N\rangle = |n, y_0\rangle$ labeled by integers $n = 0, 1, 2, \dots$, and $y_0 = \ell^2 p_x$, with wave functions of the form

$$\langle x, y | N \rangle = (L_x)^{-1/2} e^{ixp_x} \phi_n(y; y_0). \quad (2.4)$$

The $\phi_n(y; y_0)$ are highly localized around $y \sim y_0$ with spread $\Delta y \sim O(\ell)$, and are given by the usual harmonic-oscillator wave functions for electrons in the sample bulk. In what follows we shall take no explicit account of the electron edge states, which, being always extended, have little to do with field-induced delocalization.

With $\langle x, y | N \rangle$ taken to be periodic in x , $y_0 = \ell^2 p_x$ is labeled by integers k :

$$y_0 = (2\pi\ell^2/L_x)k \equiv y_0[k]. \quad (2.5)$$

We shall henceforth use this discrete label k rather than y_0 to refer directly to each electron state, with normalization $\langle N | N' \rangle = \delta_{nn'} \delta_{kk'}$.

For numerical analyses it is advantageous to handle the Hamiltonian $H_{NN'} \equiv \langle N | \mathcal{H} | N' \rangle$ in $N = (n, k)$ space:

$$H_{NN'} = \omega(n + \frac{1}{2}) \delta_{NN'} + U_{NN'} + eE_y y_{NN'}, \quad (2.6)$$

$$U_{NN'} = \frac{1}{L_x} \sum_i \lambda_i e^{-i(y_0 - y'_0)x_i/\ell^2} \phi_n(y_i; y_0) \phi_{n'}(y_i; y'_0), \quad (2.7)$$

$$y_{NN'} = \{y_0 \delta_{nn'} + \ell Y_{nn'}\} \delta_{kk'}, \quad (2.8)$$

$$Y_{nn'} = \sqrt{n'/2} \delta_{n+1, n'} + \sqrt{n/2} \delta_{n, n'+1}, \quad (2.9)$$

where $y_0 = y_0[k]$ and $y'_0 = y_0[k']$.

When the disorder $U_{NN'}$ is weak compared with the level gap, i.e., $|\lambda_i/2\pi\ell^2| < \omega$, one can diagonalize $H_{NN'}$ with respect to Landau-level labels (n, n') by a suitable unitary transformation $H^W = W H W^{-1}$. In particular, a simple $O(U)$ choice $W = e^{i\Lambda}$ with

$$i\Lambda_{NN'} = \frac{eE_y Y_{nn'} \delta_{kk'} + U_{NN'}}{\omega(n - n')} \quad (\text{for } n \neq n'), \quad (2.10)$$

leads to the Hamiltonian $\langle N | H^W | N' \rangle = \delta_{nn'} H_{nn}^W(k, k')$ governing each impurity-broadened Landau subband:

$$H_{nn}^W(k, k') = \left\{ \omega(n + \frac{1}{2}) + eE_y y_0 \right\} \delta_{kk'} + U_{nn}(k, k') + O(U^2/\omega), \quad (2.11)$$

where we have set $U_{NN'} \rightarrow U_{nn'}(k, k')$.

Numerically diagonalizing $H_{nn}^W(k, k')$, one obtains eigenstates $|\alpha\rangle$ forming the n th subband, with wave functions of the form $\langle n, k | \alpha \rangle$. Then the current density carried by an eigenstate $|\alpha\rangle$ is calculated through

$$j_x^{(\alpha)}(x, y) = e\omega \text{Re} [\langle \alpha | W | \mathbf{x} \rangle \langle \mathbf{x} | (y - y_0) W^{-1} | \alpha \rangle]. \quad (2.12)$$

Impurities capture orbiting electrons and make them localized in space. In contrast, an applied (or internally generated) Hall field causes a drift of electrons with velocity $v_x \sim E_y/B$ and works to delocalize them. A simple estimate of energy cost¹⁸ reveals how these two effects compete: Consider an impurity of strength λ placed at $x = y = 0$ on an infinite plane with $E_y = 0$. It traps an electron and in each Landau level n there arises one localized state of energy shift $\Delta\epsilon \approx \lambda/(2\pi\ell^2)$ relative to the level center $\omega(n + \frac{1}{2})$. [This is readily seen if one notes that $U_{nn}(k, k')$ in the present case is a projection to the n th level ($\propto |n\rangle \langle n|$) of a harmonic oscillator with coordinate y_0 .] It is thus convenient to define a dimensionless strength s by $\lambda/(2\pi\ell^2) = s\omega$. As a Hall field is turned on, this localized state will perceive over its spatial extent of $O(\ell)$ an energy variation of magnitude $\sim e\ell E_y$. Accordingly, if the field becomes so strong that

$$e\ell |E_y| \gtrsim |\lambda|/(2\pi\ell^2) = |s|\omega, \quad (2.13)$$

the impurity would fail to capture any electron. In the next section we shall make this criterion for delocalization quantitative by a numerical analysis.

III. THE CASE OF A SINGLE IMPURITY

Consider a sample of length $L_x = \sqrt{2\pi\ell} \times 16 \approx 40\ell$ and width $L_y = \sqrt{2\pi\ell} \times 8 \approx 20\ell$, supporting $16 \times 8 = 128$ electron states per level with $-\frac{1}{2}L_y \leq y_0 < \frac{1}{2}L_y$, or $y_0 = (2\pi\ell^2/L_x)k$ with $k = -64, -63, \dots, 63$. Place an impurity of strength $s = 0.1$ at $(x, y) = (10\ell, 0)$ in the middle of the sample and examine the electron states about the impurity by varying the field E_y or the ratio

$$R = e\ell |E_y|/s\omega. \quad (3.1)$$

It turns out that the electrons states near the boundary $y = \pm\frac{1}{2}L_y \sim \pm 10\ell$ are hardly affected by the impurity.

A close look into the $n = 0, 1, 2, 3$ levels reveals the following general features: In the n th level there arise $(n + 1)$ states of sizable spread (in y_0) $\sim O(\ell)$, all of which turn out localized when E_y is sufficiently weak (e.g., $R < 0.001$). Only one of them, having $\Delta\epsilon \approx s\omega$, is tightly localized. The other n states gain practically no energy shift $\Delta\epsilon \approx 0$ and get easily delocalized as E_y is increased, in accordance with the criterion (2.13).

In what follows we shall focus on the tightly-localized states with $\Delta\epsilon \approx s\omega$; there is one such state per level. They carry no current while E_y is sufficiently weak. For $R > 0.15$ they start carrying an appreciable amount of current $J_x^{\text{loc}} = \int dy j_x^{\text{loc}}(x, y)$, increasing with E_y on average and becoming sizable at some discrete values of E_y . Figure 1 shows such current-field characteristics for a potentially-localized state in the $n = 0$ level, along with a smooth curve interpolating through the local minima.

A direct look into current distributions shows that for these discrete values of E_y a localized state strongly interferes with an extended state nearly degenerate in energy and lying within its spatial extent. Noting that extended states are equally spaced with separation $\Delta y_0 \equiv 2\pi\ell^2/L_x$ in y_0 space, one expects that such interference takes place when $s\omega \approx eE_y \Delta y_0 \times \text{integer}$, i.e., at discrete values of the ratio R ,

$$R^{\text{disc}} \approx (\ell/\Delta y_0)/K \quad (3.2)$$

with some integers $K = 1, 2, \dots$. Indeed, the sequence

$$R^{\text{disc}} \approx 0.1705, 0.1803, 0.1913, 0.204, \dots, \quad (3.3)$$

obtained for the localized state of the $n = 0$ level is reproduced from Eq. (3.2) with $\Delta y_0 \approx 0.3133\ell$ and $K = 19, 18, 17, \dots$ to accuracy of two percent or less. Agreement becomes almost perfect if one notes that an $O(E_y^2)$ correction makes the energy $\Delta\epsilon^{\text{loc}}$ of the localized

state larger than $\lambda/(2\pi\ell^2)$ by factor $f = 1 + \frac{1}{2}R^2$ and includes this factor on the right-hand side of Eq. (3.2).

The smooth interpolating current-field curve in Fig. 1 rises from 10^{-6} to 10^{-2} as R varies from 0.23 to 0.33; this shows that delocalization proceeds abruptly over a small range of R or E_y . Actually, a simple parameterization $J_x^{\text{loc}} = -e(E_y/B)(1/L_x)F_{n=0}(R)$ with

$$F_{n=0}(R) = 1/\exp[\exp[5.264 - 11.52R]] \quad (3.4)$$

gives a good fit to the curve for $0.17 \lesssim R \lesssim 0.33$.

Because the onset of the interference is determined geometrically, the sequences R^{disc} for analogous localized states of higher levels are essentially the same as the $n = 0$ sequence, with slight deviations (of a few percent) in overall magnitude caused by the $O(E_y^2)$ correction to $\Delta\epsilon^{\text{loc}}$, which for the n th level is given by factor $f_n = 1 + (n + \frac{1}{2})R^2$. The interference, however, becomes stronger with n (because of larger spatial overlap among nearly-degenerate states) and the interpolating current-field curves rise more steeply with R , as shown in Fig. 1 for the $n = 1, 2, 3$ levels. These curves are distinct, but almost coincide by simple rescaling of the argument:

$$\begin{aligned} F_{n=0}(R) &\approx F_{n=1}(R/1.07) \\ &\approx F_{n=2}(R/1.11) \approx F_{n=3}(R/1.15), \end{aligned} \quad (3.5)$$

which holds quite well for $0.001 \lesssim F_n \lesssim 0.01$. One may define a critical ratio R^{cr} as such at which $F_n(R)$ reaches some given value, say, $1/10^3$. Then, Eq. (3.5) implies that R^{cr} decreases only by a few percent as one moves to the adjacent higher level; indeed, from Fig. 1 one can read off $R^{\text{cr}} \approx (0.29, 0.27, 0.26, 0.25)$ for $n = (0, 1, 2, 3)$. This shows that $R = e\ell|E_y|/(sw)$ is a good measure to express field-induced delocalization of electron states, with only slight reference to specific levels n .

We have made the sample twice and four times longer ($L_x \rightarrow 2L_x \rightarrow 4L_x$) and observed that $F_n(R)$ scale with L_x in such a way that $(1/L_x)F_n(R)$ stay fixed for each $n = 0, 1, 2, 3$ over the range $0.17 \lesssim R \lesssim 0.32$, giving rise to a relation analogous to Eq. (3.5). It thus appears that $F_{n=0}(R)$ has a universal meaning of its own.

IV. CASE OF RANDOM IMPURITIES

Let us next consider samples with random impurities. We earlier considered¹⁸ 180 short-range impurities of varying strength within the range $|s_i| \leq 0.1$, randomly distributed over a domain of length $\sqrt{2\pi\ell} \times 28 \approx 70\ell$ and width $\sqrt{2\pi\ell} \times 6 \approx 15\ell$. Here we shall reshuffle them and generate a new configuration of 360 impurities distributed over a domain of larger width $\approx 30\ell$; see the appendix for details. We embed this impurity configuration in the region $-15\ell \leq y \leq 15\ell$ of a Hall sample of length $L_x = \sqrt{2\pi\ell} \times 28 \approx 70\ell$ and width $L_y = \sqrt{2\pi\ell} \times 18 \approx 45\ell$, supporting $N_s = 28 \times 18 = 504$ electron states per subband with $-\frac{1}{2}L_y \leq y_0 < \frac{1}{2}L_y$. Note that the disordered

domain accommodates roughly $N_s^{\text{eff}} \approx 28 \times 12 = 336$ electrons per subband.

Of our main concern are the electron states residing over the disordered domain, that are to simulate electrons in the bulk of a realistic sample. We take no explicit account of the edge states and simply leave the two zones $15\ell < |y| \lesssim 22.5\ell$ of the sample impurity-free. In practice, to determine the electron states in the disordered bulk one has to numerically diagonalize the Hamiltonian for a sample of somewhat larger width like this.

For each subband n we arrange the electron states in the order of descending energy and use the number of vacant states, N_v , to specify the filling of the subband. For convenience we start with the filled subband ($N_v = 0$) and study the total current this subband supports,

$$J_x = \int dy \sum_{\alpha} j_x^{(\alpha)}(x, y), \quad (4.1)$$

by removing electrons one by one. In Fig. 2(a) we plot J_x as a function of N_v for the $n = 0$ subband and $R = 10^{-4}, 0.001, 0.01, 0.025, 0.05, 0.1, 0.2$, where

$$R \equiv -e\ell E_y/(0.1\omega) \quad (4.2)$$

is now normalized using $|s|_{\text{max}} \equiv \text{Max}\{|s_i|\} = 0.1$. There, simply for ease of exposing numerical results we have focused on 437 electron states whose center positions $\langle \alpha | y | \alpha \rangle$ lie across the region $|y| < 19.6\ell$; the electron states residing outside are close to undisturbed modes.

Let us first look at the $R = 10^{-4}$ case, where the upper and lower plateaus are clearly seen for $0 \leq N_v \lesssim 170$ and $270 \leq N_v$, respectively, supporting about 330 localized states in total. There the linear decrease of J_x for $170 \lesssim N_v \lesssim 210$ and $230 \lesssim N_v \lesssim 270$ is due to gradual evacuation of extended states from the impurity-free zones $|y| \gtrsim 15\ell$. A steep fall of J_x around $N_v \sim 220$ indicates that a large portion of the Hall current is carried by a small number of states residing in the sample bulk.

The plateaus shrink rapidly with increasing $|E_y|$, and become hardly visible for $R = 0.2$ in Fig. 2(a). Somewhat unexpectedly, the way the upper and lower plateaus diminish with increasing R is virtually the same for higher $n = 1, 2, 3$ subbands as well, as shown in Fig. 2(b) for the $n = 2$ subband. Numerically, the number of states forming the plateaus, N^{pl} , decreases exponentially with R , with little dependence on $n = 0, 1, 2, 3$, as seen from Fig. 2(c); $N^{\text{pl}} \approx 330 e^{-R/0.041}$ gives a good numerical fit.¹⁹

As seen from Fig. 2(a), a filled subband carries the same amount of Hall current as in the impurity-free case. One may thus simply look into the uppermost occupied subband in studying the dependence of the Hall current on the Hall field.

In Fig. 2(b) the plateaus are somewhat blurred when E_y is very weak, $R \lesssim 10^{-3}$. This blur or instability is due to the interference among nearly degenerate states and

grows prominent in higher subbands, especially in the regime of small R , where J_x itself gets small. Such blur makes N^{pl} underestimate the actual plateau width, and this explains why apparent deviations from the universal $N^{\text{pl}} - R$ characteristic develop for small R in Fig. 2(c).

We have so far supposed changing the filling fraction $\nu = N_e/N_s$ of Landau subbands by varying electron population N_e with B kept fixed. Let us next consider what would happen if one reaches higher subbands by reducing B while keeping N_e fixed, as commonly done in experiments. Unfortunately it is impractical to change the length unit $\ell = 1/\sqrt{eB}$ continuously in numerical simulations. We shall therefore take an indirect route and examine what happens if the magnetic field is changed from B_0 to B_0/κ . We suppose that the sample size²⁰ is defined in units of $\ell_0 = 1/\sqrt{eB_0}$ of the original field B_0 . Then, as B is varied, the disordered domain accommodates about $N_s^{\text{eff}} \approx 336/\kappa$ states per subband so that $N_{\text{imp}}/N_s^{\text{eff}} \approx \kappa$. Thus, reducing the magnetic field $B_0 \rightarrow B_0/\kappa$ not only attains a larger filling factor $\nu \rightarrow \kappa\nu$ but also effectively makes impurities κ times denser.

Some remarks are in order here. We have so far counted the number of localized states through the plateau width N^{pl} , which best visualizes how the Hall plateaus shrink with R . This N^{pl} , however, tends to overlook (a small portion of) localized states hidden off the plateaus and becomes less reliable for large R , where N^{pl} gets small. Fortunately there is another measure, less direct but better suited for detecting the disappearance of Hall plateaus: One can directly count the number N^{loc} of states that carry an almost vanishing amount of current per state, e.g., less than 1% of the unit $(-e/L_x)E_y/B$. (We adopt this choice of 1% below.)

Figure 3(a) shows N^{loc} of the uppermost subband, plotted as a function of $R \propto e\ell|E_y|/\omega$, for various choices of $B = B_0/\kappa$ with $\kappa = 0.33 \sim 4$. Actually the data refer specifically to the $n = 0$ subband but, in view of what we have learned from the fixed- B cases, we suppose that they apply to higher subbands as well. One may thus regard, e.g., the $\kappa = 2$ curve as referring to the $n = 1$ subband (or the spin-split $n = 0$ subband if the electron spin is taken into account) with $1 < \nu \leq 2$, which is reached from the $\kappa = 1$ curve referring to the $n = 0$ subband with $0 < \nu \leq 1$ by reducing $B = B_0 \rightarrow \frac{1}{2}B_0$.

Figure 3(b) tells us that, in the regime of dense impurities $N_{\text{imp}}/N_s^{\text{eff}} \approx \kappa \gtrsim 1$, the $N^{\text{loc}} - R$ curves appear quite universal, exhibiting, like N^{pl} , an exponential fall-off over a wide range $R \gtrsim 0.1$, with slight dependence on κ for its range of change $1 \leq \kappa \leq 4$. The apparent deviations, growing with κ for $R < 0.1$, are due to the interference among nearly degenerate states. Thus, an approximate scaling law of the form

$$N^{\text{loc}} \approx N_0 e^{-R/0.058}, \quad (4.3)$$

with $N_0 \approx N_{\text{imp}} = 360$, determines how N^{loc} depends on E_y and B over a wide range $R \gtrsim 0.1$.

As for the normalization N_0 it is clear that $N_0 \propto N_{\text{imp}}$ in general, and that $N_0 \approx N_{\text{imp}}$ when $N_{\text{imp}} \approx N_s^{\text{eff}}$,

in which case all impurities are expected to capture electrons in the $E_y \rightarrow 0$ limit. It is remarkable that $N_0 \approx N_{\text{imp}}$ holds well even though the ratio $N_{\text{imp}}/N_s^{\text{eff}}$ far exceeds unity in Fig. 3(b).

The situation somewhat changes in the regime of dilute impurities, $N_{\text{imp}}/N_s^{\text{eff}} < 1$. See Fig. 3(a) and (c). There, as impurities become dilute ($\kappa = 1 \rightarrow 0.33$), N^{loc} rises more rapidly with reducing R and tends to saturate for $R \sim 0$; this is because all the impurities would capture electrons before R reaches zero. Thus, for dilute impurities $N_{\text{imp}}/N_s^{\text{eff}} \ll 1$, the $N^{\text{loc}} - R$ characteristics significantly deviate from the scaling form (4.3). Still the values of N^{loc} in the near-breakdown regime ($R = 0.25 \sim 0.4$) stay roughly the same, and actually are consistent with those of the $N_{\text{imp}}/N_s^{\text{eff}} > 1$ case.

A physical picture suggested by this stability of N^{loc} for large R is that the electron states remaining localized in the near-breakdown regime are always governed by the same set of impurities of large strength $|s_i| \sim |s|_{\text{max}}$; that is, one always encounters the same set of localized states in the near-breakdown regime. If this is the case, weaker impurities ($|s_i| \ll |s|_{\text{max}}$) would be irrelevant to the onset of the breakdown.

To test this picture we have examined the case of a truncated impurity configuration where only 180 impurities of strength $0.05 \leq |s_i| \leq 0.1$ are retained, with the weaker ones suppressed. The resulting $N^{\text{loc}} - R$ characteristics, plotted with unfilled symbols in Fig. 3(d) for $\kappa = 1, 2, 3, 4$, are indeed consistent with those of the original $N_0 \approx N_{\text{imp}} = 360$ case for $R \gtrsim 0.25$. Further truncation of impurities into an even smaller range $0.075 \leq |s_i| \leq 0.1$ entails no essential change. This supports our picture and implies that for a general impurity configuration N_0 is not simply given by N_{imp} but by the effective number of impurities extrapolated from the density of strong impurities ($|s_i| \sim |s|_{\text{max}}$). We have also examined a number of cases with $N_{\text{imp}} = 180$ and 720, and arrived at essentially the same conclusion.

A practical way to define the disappearance of a Hall plateau is to refer to a critical value of E_y at which N^{loc} or the ratio N^{loc}/N_e reaches a certain prescribed number. Then, it follows from the universal $N^{\text{loc}} - R$ characteristic in the near-breakdown regime that the critical field scales like $e\ell|E_y^{\text{cr}}|/(0.1\omega) = C = \text{const.}$, i.e.,

$$e|E_y^{\text{cr}}| = |s|_{\text{max}} C \omega/\ell \propto B^{3/2}, \quad (4.4)$$

where we have isolated the dependence of E_y^{cr} on the sample-specific impurity strength $|s|_{\text{max}}$. It is understood that $|s|_{\text{max}}$ now refers to a typical strength of (strong) impurities relevant in the near-breakdown regime.²¹ The scaling law $|E_y^{\text{cr}}| \propto B^{3/2}$ applies to each spin-split subband reached by varying B .

To get an idea of the magnitude $|E_y^{\text{cr}}$ let us look at Fig. 3(b) and choose $C \approx 0.25$, for which we count only 10 localized states in the uppermost subband. This leads to a critical field of magnitude $|E_y^{\text{cr}}| \sim 250 \text{ V/cm}$ at the $\nu = 1$ plateau for typical values $\omega \approx 10 \text{ meV}$ and $\ell \approx$

100 Å, with $|s|_{\max} = 0.1$. Critical fields of this order of magnitude appear to be consistent with experiments.¹¹

There are some testable consequences of the scaling law. First it is of interest to study how the Hall-plateau width depends on ν and E_y . Let $B^{(\nu=1)}$ denote the value of B at which the lowest subband is filled up, so that one can write the filling factor as $\nu = B^{(\nu=1)}/B$. Let us suppose that each subband contains the same number of localized states $\sim \frac{1}{2}N^{\text{loc}}$ in its upper and lower halves of the spectrum. Then a plateau develops near integer filling $\nu \sim n$ if $|nN_s - N_e| \leq \frac{1}{2}N^{\text{loc}}$ is satisfied; i.e., the plateau lies over the range $\nu_- \leq \nu \leq \nu_+$ with ν_{\pm} determined from $n/\nu_{\pm} = 1 \mp \frac{1}{2}N^{\text{loc}}(\nu_{\pm}; E_y)/N_e$, where N^{loc} depends on ν and E_y . When E_y is very weak and localization is almost complete, i.e., $N^{\text{loc}} \rightarrow N_s$, this leads to $\nu_{\pm} \approx n \pm \frac{1}{2}$ so that the plateau width

$$\Delta\nu \equiv \nu_+ - \nu_- \approx 1 \quad (4.5)$$

at each plateau, as observed experimentally²² at low temperatures. [The observation²² of sharp steps connecting the plateaus would suggest that the case of dense impurities $N_{\text{imp}}/N_s > 1$ applies to realistic samples.]

In contrast, in the near-breakdown regime $N^{\text{loc}}/N_e \ll 1$ (or for large E_y) we find from Eq. (4.3) the plateau width $\Delta B/B^{(\nu=1)} \equiv 1/\nu_+ - 1/\nu_-$ of the form

$$\Delta B \approx \frac{1}{n} B^{(\nu=1)} (N_0/N_e) e^{-\xi n^{3/2} E_y} \quad (4.6)$$

around $\nu \sim n$, where $\xi = (C/0.058)/E_y^{\text{cr}(\nu \sim 1)}$ refers to the critical field $E_y^{\text{cr}(\nu \sim 1)}$ at the $\nu = 1$ plateau. Thus, near the breakdown the width ΔB scales like $(1/n)e^{-\xi n^{3/2} E_y}$ at $\nu \sim n$ plateaus. A close look into how the width ΔB decreases with E_y at different plateaus will reveal another manifestation of the $E_y^{\text{cr}} \propto B^{3/2}$ law.

The number of visible plateaus is readily determined also. Suppose that the total current J_x is kept fixed while B is varied, as normally done in experiments. Let $J_x^{\text{cr}(\nu \sim 1)}$ denote the critical current at which the $\nu \sim 1$ plateau disappears. Then the critical current at the $\nu \sim n$ plateau scales with n like $J_x^{\text{cr}(\nu \sim n)} = n^{-1/2} J_x^{\text{cr}(\nu \sim 1)}$. As a result, for given J_x one will observe n_{\max} plateaus, while reducing B , where n_{\max} denotes the largest integer satisfying the equation

$$n < (J_x^{\text{cr}(\nu \sim 1)}/J_x)^2. \quad (4.7)$$

V. SUMMARY AND DISCUSSION

In this paper we have studied the competition of the Hall field with disorder in triggering the breakdown of the QHE. In the case of a single impurity we have seen that field-induced delocalization of a localized state starts with its interference with nearly-degenerate extended

states. This geometrical nature of the onset and subsequent abrupt growth make the delocalization process, when expressed in terms of $e\ell E_y/B$, practically independent of the Landau-subband index n . Such n independence is largely carried over to the case of random impurities. We have seen, in particular, that in the regime of dense impurities $N_{\text{imp}}/N_s > 1$ (which presumably applies to realistic samples) the number of localized states, decreasing exponentially with $|E_y|$, obeys an approximate scaling law written in terms of $e\ell E_y/\omega \propto E_y/B^{3/2}$. Deviations from the scaling form arise in the regime of dilute impurities. Nevertheless the results of our numerical analysis are neatly summarized in a physical picture that the breakdown is controlled by a fixed set of impurities of large strength $|s_i| \sim |s|_{\max}$, that support localized states in the near-breakdown regime. This picture offers a simple explanation for the empirical $E_y^{\text{cr}} \propto B^{3/2}$ law of the critical breakdown field, and leads to some testable consequences concerning the number and widths of visible Hall plateaus. It is also consistent with the observation of Cage *et al.*⁷ that the breakdown of the dissipationless current is spatially inhomogeneous.

Experimentally the $E_y^{\text{cr}} \propto B^{3/2}$ law is established not only for each specific sample but also for samples differing in carrier density and mobility.¹¹ This experimental fact indicates that the critical field E_y^{cr} is practically independent of both electron concentration $\propto N_e$ and impurity concentration $\propto N_{\text{imp}}$. This is consistent with the above-mentioned physical picture or its outcome in Eq. (4.4), where the critical field, though sensitive to the characteristic strength $|s|_{\max}$ of disorder, appears practically independent of N_e and N_{imp} . The $|s|_{\max}$ is related to the width of each subband. Its magnitude $|s|_{\max} \sim O(0.1)$ differs from a sample to another, but its range of variation is presumably of $O(1)$, far smaller than the ranges of variations of sample-specific electron and impurity concentrations. The observed $E_y^{\text{cr}} \propto B^{3/2}$ law would thus be attributed to relatively small variations in $|s|_{\max}$ for a variety of samples. It is also a natural consequence of the present *intrasubband* process that the magnitude of E_y^{cr} falls within the observed range of a few hundred V/cm, one order of magnitude smaller than what intersubband processes¹⁴⁻¹⁶ typically predict.

We have used a uniform field E_y to detect the current-carrying characteristics of Hall electrons. In real samples the Hall field generated by an injected current is not necessarily uniform and has actually been observed to be stronger near the sample edges.²³ Under such general circumstances the field E_y employed in our analysis should refer to the smallest of local averages of the Hall field in the sample bulk.

ACKNOWLEDGMENTS

The author wishes to thank S. Kawaji for useful discussions. This work is supported in part by a Grant-in-Aid

for Scientific Research from the Ministry of Education of Japan, Science and Culture (No. 10640265).

APPENDIX A: IMPURITY DISTRIBUTION

In this appendix we describe how to construct the configuration of 360 random impurities used in Sec. IV. We earlier used a configuration $P_{180} = \{(\bar{x}_i, \bar{y}_i, s_i), i = 1, \dots, 180\}$ of 180 impurities of strength s_i located at (\bar{x}_i, \bar{y}_i) randomly distributed over the range $0 \leq \bar{x} \leq 24$, $0 \leq \bar{y} \leq 6$ and $|s_i| \leq 0.1$. Generate out of this P_{180} another set $P'_{180} = \{(\bar{x}_{i+180}, \bar{y}_{i+180}, s_{i+180}), i = 1, \dots, 180\}$ via a shift $(10, 2, 0.08)$ [which is our arbitrary choice] and rearrangement so that $\bar{x}_{i+180} = \bar{x}_i + 10 \bmod 24$, $\bar{y}_{i+180} = \bar{y}_{181-i} + 2 \bmod 6$, and $s_{i+180} = s_i + 0.08 \bmod 0.2$, within the range $0 \leq \bar{x} < 24$, $0 \leq \bar{y} < 6$ and $|s_i| \leq 0.1$.

Then shift P_{180} by $(0, -6, 0)$ and combine it with P'_{180} to form a set P_{360} of 360 impurities distributed over the wider range $0 \leq \bar{x} \leq 24$ and $-6 \leq \bar{y} \leq 6$. Finally, via rescaling $x_i = \sqrt{2\pi\ell} \times (28/24) \times \bar{x}_i$ and $y_i = \sqrt{2\pi\ell} \times \bar{y}_i$ we distribute these 360 impurities at positions (x_i, y_i) over the domain $0 \leq x \lesssim 70\ell$ and $-15\ell \lesssim y \lesssim 15\ell$.

- ¹² A. Boisen, P. Boggild, A. Kristensen, and P. E. Lindelof, Phys. Rev. B **50**, 1957 (1994).
- ¹³ T. Shimizu, T. Okamoto, and S. Kawaji, Physica B **249-251**, 107 (1998)
- ¹⁴ D. C. Tsui, G. J. Dolan, and A. C. Gossard, Bull. Am. Phys. Soc. **28**, 365 (1983).
- ¹⁵ O. Heinonen, P. L. Taylor, and S. M. Girvin, Phys. Rev. B **30**, 3016 (1984).
- ¹⁶ L. Eaves and F. W. Sheard, Semicond. Sci. Technol. **1**, 346 (1986).
- ¹⁷ V. Nikos Nikopoulos and S. A. Trugman, Phys. Rev. Lett. **65**, 779 (1990).
- ¹⁸ K. Shizuya, Phys. Rev. B **59**, 2142 (1999); see also, Phys. Rev. Lett. **73**, 2907 (1994).
- ¹⁹ To define N^{pl} we have allowed a small deviation and counted the number of states that satisfy the cutoff $|J_x - (\text{plateau values})| < 0.5$ unit of $(-e/L_x)E_y/B$.
- ²⁰ In units of $\sqrt{2\pi\ell}$ the sample size is $(28/\sqrt{\kappa}) \times (18/\sqrt{\kappa})$, which we approximate by some appropriate integers so that the number of states N_s takes an integer. In what follows, we actually take $28/\sqrt{\kappa} \approx (23, 20, 16, 14)$ and $18/\sqrt{\kappa} \approx (15, 13, 12, 10)$ for $\kappa = (1.5, 2, 3, 4)$, respectively. Similarly, for $\kappa = (0.67, 0.5, 0.33)$ we take the length to be $(34, 40, 48)$ and width to be $(20, 22, 26)$, respectively.
- ²¹ Note here that $s_i = \lambda_i/(2\pi\ell^2\omega) = \lambda_i m^*/(2\pi)$ are independent of the magnetic field B (as long as λ_i are).
- ²² M. A. Paalanen, D. C. Tsui, and A. C. Gossard, Phys. Rev. B **25**, 5566 (1982).
- ²³ P. F. Fontein *et al.*, Phys. Rev. B **43**, 12 090 (1991).

- ¹ K. von Klitzing, G. Dorda, and M. Pepper, Phys. Rev. Lett. **45**, 494 (1980); D. C. Tsui, H. L. Stormer, and A. C. Gossard, *ibid.* **48**, 1559 (1982).
- ² For a review, see *The Quantum Hall Effect*, edited by R. E. Prange and S. M. Girvin (Springer-Verlag, Berlin, 1987).
- ³ H. Aoki and T. Ando, Solid State Commun. **38**, 1079 (1981). See also T. Ando, Y. Matsumoto, and Y. Uemura, J. Phys. Soc. Jpn. **39**, 279 (1975).
- ⁴ R. E. Prange, Phys. Rev. B **23**, 4802 (1981).
- ⁵ R. B. Laughlin, Phys. Rev. B **23**, 5632 (1981).
- ⁶ G. Ebert, K. von Klitzing, K. Ploog, and G. Weimann, J. Phys. C **16**, 5441 (1983).
- ⁷ M. E. Cage, R. F. Dziuba, B. F. Field, E. R. William, S. M. Girvin, A. C. Gossard, D. C. Tsui, and R. J. Wagner, Phys. Rev. Lett. **51**, 1374 (1983).
- ⁸ H. L. Stormer, A. M. Chang, D. C. Tsui, and J. C. M. Hwang, Proc. 17th Int. Conf. Physics of Semiconductors, San Francisco, 1984, ed. J. D. Chadi and W. A. Harrison (Springer Verlag, New York, 1985) p. 267.
- ⁹ S. Komiyama, T. Takamasu, S. Hiyamizu, and S. Sasa, Solid State Commun. **54**, 479 (1985).
- ¹⁰ N. Q. Balaban, U. Meirav, H. Shtrikman, and Y. Levinson, Phys. Rev. Lett. **71**, 1443 (1993).
- ¹¹ S. Kawaji, K. Hirakawa, M. Nagata, T. Okamoto, T. Fukase, and T. Gotoh, J. Phys. Soc. Jpn. **63**, 2303 (1994); T. Okuno, S. Kawaji, T. Ohru, T. Okamoto, Y. Kurata, and J. Sakai, *ibid.* **64**, 1881 (1995); S. Kawaji, Semicond. Sci. Technol. **11**, 1546 (1996).

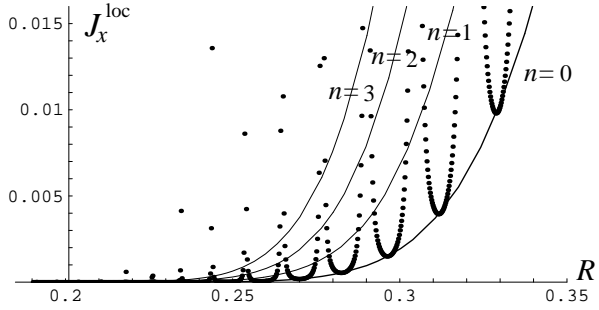


FIG. 1. A potentially localized state of the $n = 0$ level carries an amount of current J_x^{loc} [plotted in units of $-(e/L_x)E_y/B$], that becomes sizable at some discrete values of $R = e\ell|E_y|/s\omega$, with a smooth curve interpolating through the local minima. Also shown are analogous interpolating current-field curves for the localized states of the $n = 1, 2, 3$ levels.

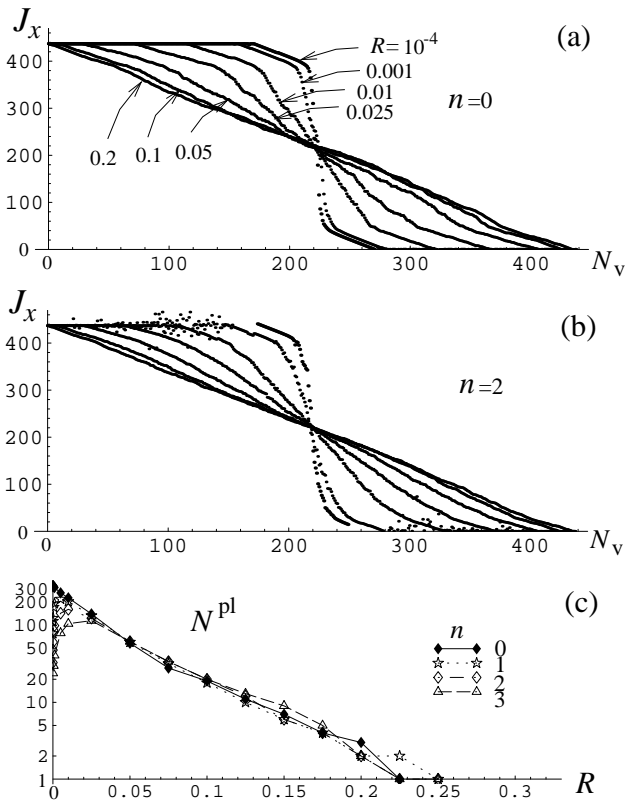


FIG. 2. (a) The Hall current J_x carried by the $n = 0$ subband [in units of $-(e/L_x)E_y/B$] vs vacancy N_v for $R \equiv e\ell|E_y|/|s|_{\text{max}}\omega = 0.0001, 0.001, 0.01, 0.025, 0.05, 0.1, 0.2$. (b) J_x vs N_v for the $n = 2$ subband. The blur about the plateaus shown is associated with the $R = 0.001$ case, and the $R = 10^{-4}$ curve is only partially shown. (c) The plateau width N^{pl} decreases exponentially with R , as shown in a $\log N^{\text{pl}}$ vs R plot for the $n = 0, 1, 2, 3$ subbands. The lines joining the data points are meant to guide the eye.

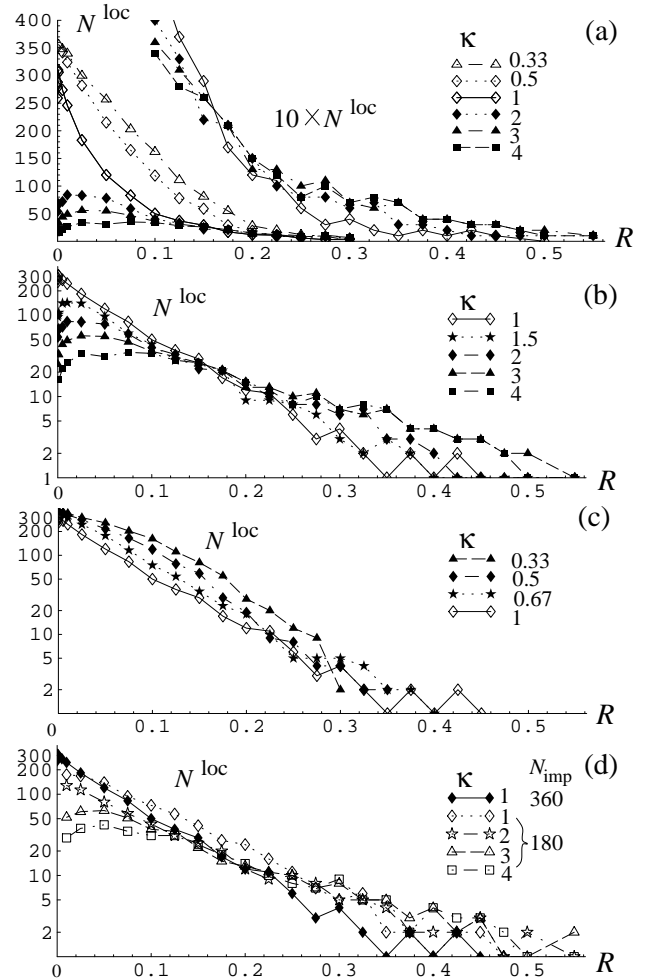


FIG. 3. The number of localized states per subband, N^{loc} , plotted as a function of $R = e\ell|E_y|/|s|_{\text{max}}\omega$. (a) N^{loc} vs R with $\kappa = 0.33 \sim 4$; $10 \times N^{\text{loc}}$ shown for $R \geq 0.1$. (b) $\log N^{\text{loc}}$ vs R with $\kappa = 1, 1.5, 2, 3, 4$. (c) $\kappa = 1, 0.67, 0.5, 0.33$. (d) $\log N^{\text{loc}}$ vs R for a truncated configuration with only 180 impurities of strength $0.05 \leq |s_i| \leq 0.1$ kept.